Multiple Changes of Order of the Vortex Melting Transition in $Bi_2Sr_2CaCu_2O_8$ with Dilute Columnar Defects

T. Verdene,[1,*] H. Beidenkopf,[1] Y. Myasoedov,[1] H. Shtrikman,[1] M. Rappaport,[1] E. Zeldov,[1] and T. Tamegai[2]

[1]*Department of Condensed Matter Physics, Weizmann Institute of Science, Rehovot 76100, Israel*

[2]*Department of Applied Physics, The University of Tokyo, Hongo, Bunkyo-ku, Tokyo 113-8656, Japan*

(Received 3 January 2008; published 8 October 2008)

A low concentration of columnar defects is reported to transform a first-order vortex lattice melting line in $Bi_2Sr_2CaCu_2O_8$ crystals into alternating segments of first- and second-order transitions separated by two critical points. As the density of columnar defects is increased, the critical points shift apart and the range of the intermediate second-order transition expands. The measurement of equilibrium magnetization and the mapping of the melting line down to 27 K was made possible by employment of the shaking technique.

DOI: 10.1103/PhysRevLett.101.157003 PACS numbers: 74.25.Qt, 64.70.dg, 74.25.Dw, 74.72.Hs

The interplay between different energy scales of a physical system can induce phase transitions and yield a rich phase diagram. In particular, in a clean system a melting transition results from the competition between elasticity and thermal fluctuations and is usually of a first-order (FO) nature. The presence of a third competing scale due to disorder may suppress it to second-order (SO) and lead to a richer picture, the understanding of which is quite limited [1,2]. In order to gain insight into the competing mechanisms, we introduce an additional control parameter in the form of a variable weak correlated disorder. We report an exceptionally intricate case, where the initially FO melting transition of the vortex matter in a high temperature superconductor exhibits a rare three-section FO-SO-FO behavior and even seems to undergo a four-section FO-SO-FO-SO sequence. Our findings reveal that a SO transition is nucleated in a small segment along the FO transition line, bound by two critical points. This SO segment grows when the control parameter is increased providing insight into the general mechanism of transformation of a FO transition into a SO transition.

$Bi_2Sr_2CaCu_2O_8$ (BSCCO) high-T_c superconductor has an especially rich vortex matter phase diagram which results from the interplay between the elasticity, thermal fluctuations, and point disorder. It consists of a FO melting line [3] which separates the low-field Bragg glass from the high-field disordered phases [4–6]. At high temperatures the FO melting transition is mainly thermally driven. At lower temperatures it gradually changes into a disorder-driven inverse melting transition [7–9]. Indications of an additional almost vertical SO glass transition line at intermediate temperatures were also found [10].

This picture changes entirely with introduction of a fourth energy scale due to dense columnar defects (CDs) $B_\phi \gg B_m(T)$, where $B_\phi \equiv n_{\rm cd}\phi_0$, $n_{\rm cd}$ is the density of CDs, ϕ_0 is the flux quantum, and $B_m(T)$ is the melting field. Compared to the pinning energy to CD, the elastic energy becomes negligible. As a result, the ordered solid phase is replaced by a disordered Bose glass (BOG) phase in which vortices are localized on CDs and melt through a SO BOG transition [6,11].

In this paper we focus on the dilute CD limit, where vortices outnumber CDs at most relevant fields. Remarkably, in this limit the energy due to correlated pinning is comparable to the other three energy scales. Consequently, the four relevant energy scales mold together a particularly complex B-T phase diagram whose nature is not well understood. Most experimental [12–16], theoretical [17–20], and numerical studies [21–23] agree that at high temperatures the transition remains FO. At intermediate temperatures where the melting occurs at intermediate fields $B_m \gtrsim B_\phi$, the pristine Bragg glass phase is replaced by a porous solid with the majority of CDs occupied by strongly pinned vortices that form an amorphous matrix. The remaining vortices form ordered crystallites that are embedded in the pores of the rigid matrix [14–23]. These vortex nanocrystals melt into nanodroplets apparently through a second-order transition.

Experimentally, even a low density of CDs enhances hysteretic effects throughout most of the solid phase in BSCCO [12,13]. This is a major obstacle in mapping the true thermodynamic phase transitions of vortex matter. Lacking access to the thermodynamic behavior, past experimental studies have focused on dynamics [12–14,16,24]. It was concluded that the high temperature FO transition line terminates at a critical point (CP) whose location depends on CD density [13–16], consistent with theory and simulations [18–23]. At temperatures below the CP, however, these out-of-equilibrium studies could not evaluate the exact nature of the transition. Thus, a SO transition was premised to exist at all temperatures below the CP [13,14,19–23], though other theoretical scenarios were also considered [18]. This incomplete understanding of the dilute pinning limit led naturally to the assumption that as CD density is increased, the SO nature of melting spreads from low temperatures to higher ones with a shift

of a single CP. Our findings, however, suggest an essentially different process.

In this study we mapped for the first time the *equilibrium* phase diagram of vortex matter with dilute CDs by performing local magnetization measurements during vortex shaking. This method [7,10,25,26] utilizes an in-plane ac shaking field which agitates the vortices and assists them to assume their equilibrium positions. Tilting the magnetic field away from the CDs was shown to alter the equilibrium magnetization in YBCO crystals [27]. In contrast, in BSCCO a moderate in-plane field has essentially no effect on the equilibrium properties even in presence of CDs due to the very high anisotropy [16,28]. As a result, the ac in-plane field enhances vortex relaxation without altering the thermodynamic transitions [16]. We measured three BSCCO samples with slightly differing anisotropies, irradiated at GANIL, Caen, France with matching fields of $B_\phi = 5$, 10, 20 G and critical temperatures of 90 to 92 K, and an additional sample with $B_\phi = 20$ G and $T_c \approx 91$ K. Half of each sample was masked during irradiation to allow a direct comparison between pristine and irradiated behavior. The local magnetic induction of the sample was measured by an array of Hall sensors 10×10 μm^2 each, while sweeping the external magnetic field H at a constant temperature. Simultaneous measurements of the transition on the pristine halves of the samples show that it remained FO at all temperatures. Shaking fields up to 350 Oe at 10 Hz were used that enabled detection of a melting transition down to 27 K.

Figures 1(a)–1(c) present the measured local magnetization B-H at (a) 90 K, (b) 84 K, and (c) 42 K in $B_\phi = 10$ G sample. A FO transition appears as a sharp step in $B(H)$ and a SO transition is manifested by a break in its slope. Figure 1(d) shows the height of the measured step in the induction ΔB at the FO transitions as a function of temperature. The corresponding entropy change per vortex per double CuO_2 layer (from the Clausius-Clapeyron relation) $\Delta S = -\frac{d\phi_0}{4\pi}\frac{\Delta B}{B_m}\frac{dB_m}{dT}$ is presented in Fig. 1(e). Here $d = 15$ Å is the interlayer spacing.

To better resolve the nature of the transition we differentiated the measured induction B with respect to the applied field H. Figure 2 shows the derivatives dB/dH at representative (a) high, (b) intermediate, and (c) low temperatures. A peak in the derivative signifies a FO transition. A discontinuity indicates a SO transition. At high temperatures we find that the transition remains FO in the presence of CDs, similarly to that in the pristine areas, as previously reported [13,14]. Accordingly, $B(H)$ in Fig. 1(a) shows a sharp step, and the derivatives dB/dH in Fig. 2(a) display δ-like peaks. At a slightly lower temperature thermal fluctuations are weaker, the effective pinning potential of the CDs gains strength, and irreversibility is greatly enhanced, thus masking the underlying phase transition. We overcame this problem by applying the shaking method rendering a reversible magnetization [7,10,25,26]. Figures 1(b) and 2(b) thus show equilibrium measurements

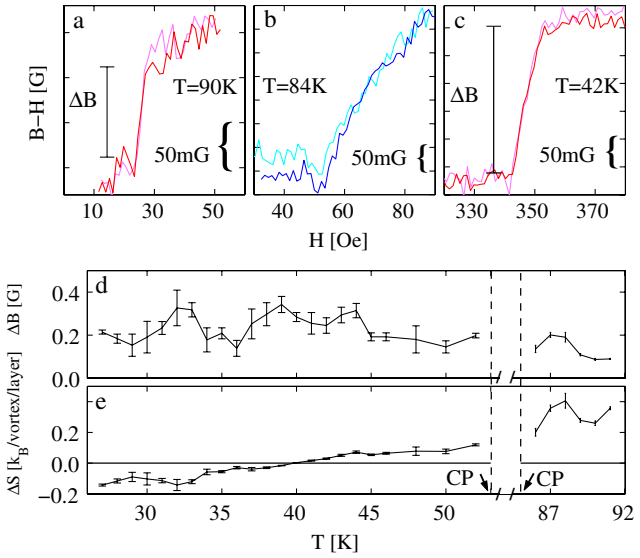

FIG. 1 (color online). Local magnetization B-H of the $B_\phi = 10$ G sample in the presence of shaking, measured upon ascending (dark) and descending (light) external field at constant temperatures of (a) 90 K, (b) 84 K, and (c) 42 K. A linear slope was subtracted for clarity. The steps in the local induction ΔB in (a) and (c) signify a FO transition. In (b), a break in the slope indicates a SO transition. (d) and (e): temperature dependence of ΔB and entropy change ΔS, respectively.

at an intermediate temperature of B-H and dB/dH, respectively. A break in the slope of the induction is clearly resolved along both ascending and descending field sweeps and the derivatives display a step structure indicating a SO transition.

Yet, our main finding is the recovery of the FO thermodynamic phase transition at lower temperatures. This is clearly visible in Fig. 1(c) as a reversible discontinuity in magnetization $B(H)$ and accordingly, in Fig. 2(c) a sharp peak in the derivatives dB/dH. This recurrence of the FO nature of the transition has been predicted theoretically [18], but has never been observed experimentally.

These findings can be explained by the following comparison of energy scales. At high temperatures thermal fluctuations are dominant enough to weaken the effective pinning potential due to CDs [13–23,29], resulting in a FO transition similar to that found in pristine samples. At intermediate temperatures, as correlated pinning gains dominance, the randomly distributed CDs alter the *equilibrium* vortex matter state, in addition to enhancing irreversible hysteretic behavior. At these temperatures the melting occurs at intermediate fields $B_m \gtrsim B_\phi$ and the pristine Bragg glass phase is replaced by a porous solid with crystallites of interstitial vortices imbedded in the pores of a rigid amorphous vortex matrix [14–16]. The size of the nanocrystals within each pore is only several times their lattice constant. These dilute nanocrystals seem to melt into nanodroplets through a SO transition probably since the range of correlations is cut off by the finite size of the pores, consistent with recent numerical simulations

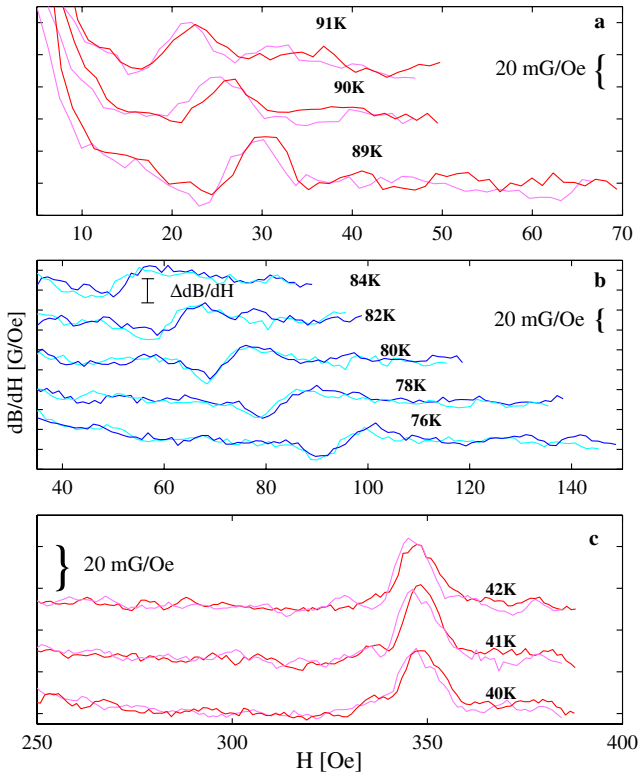

FIG. 2 (color online). The derivative of the measured induction with respect to applied field, dB/dH, of the $B_\phi = 10$ G sample in presence of shaking, measured upon ascending (dark) and descending (light) field at constant temperatures of (a) 89–91 K, (b) 76–84 K, and (c) 40–42 K. Data are shifted vertically for clarity. A peak in dB/dH in (a) and (c) signifies a FO transition, whereas a step in (b) indicates a SO transition.

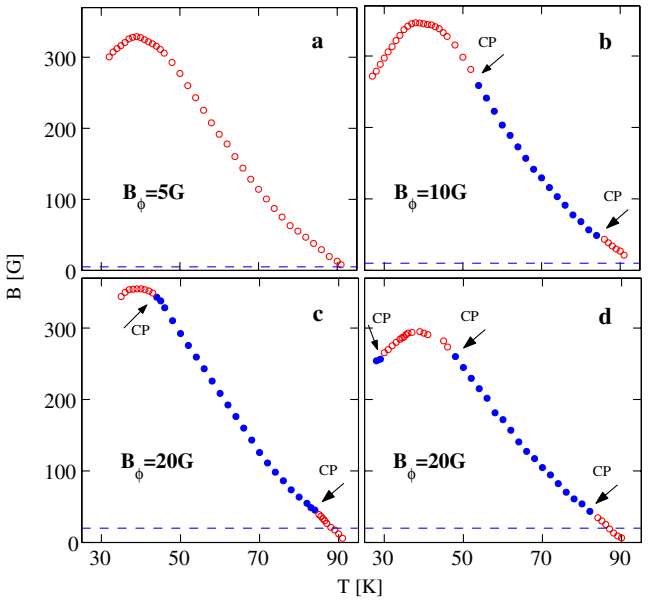

FIG. 3 (color online). Phase diagrams of irradiated BSCCO crystals showing FO (○) and SO (●) transitions. (a) In the $B_\phi = 5$ G sample the transition is FO at all temperatures. (b) For $B_\phi = 10$ G a FO-SO-FO behavior is found. (c) The SO segment expands in the $B_\phi = 20$ G sample. (d) A different $B_\phi = 20$ G sample with lower doping that exhibits a FO-SO-FO-SO sequence. The values of B_ϕ are shown by dashed lines.

[20–23]. This is similar to the dense-CD limit, where correlated pinning dominates and vortex matter undergoes a second-order BOG transition.

At low temperatures ~40 K the transition occurs at high fields. Each pinned vortex is surrounded by tens of interstitial vortices and the solid phase is increasingly dominated by inter vortex interactions [18], resulting in relatively ordered dense vortex crystallites [15]. Consequently, their melting into nanodroplets is accompanied by a discontinuity in the entropy that reflects the sharp difference in ordering of the two phases. The FO nature of the transition is thus restored, as in pristine samples.

The location and nature of the transition of the four samples was measured and mapped as summarized in Fig. 3. In all four irradiated samples, the location of the melting line remained similar to that of the pristine parts of the samples, with a maximum at ~40 K. The 5 G sample exhibits a FO transition at all temperatures. As the density of CDs is increased, more of the B-T phase space becomes dominated by correlated disorder and consequently, a larger portion of the transition line becomes SO (solid circles). The 10 and 20 G samples both display two CPs with a FO-SO-FO sequence. In the 20 G sample the two CPs are shifted further apart than in the 10 G sample and the SO transition spreads to high and low temperatures. We suggest that this trend persists until a full SO BOG transition line is attained in the dense-CD limit. Note that previous dynamic measurements [14] have found a delocalization line that separates between the nanoliquid and the homogeneous vortex liquid. This delocalization line merges with the melting line in the vicinity of the lower CP giving rise to a kink in the melting line visible in Fig. 3.

Interestingly, in the SO region dB/dH takes a more intricate shape [Fig. 2(b)]; rather than a simple upward jump, it first decreases, then jumps up and finally slightly decreases again. This structure may be explained by the association of the step in the derivative at the SO transition with the relative ordering of the two phases across the transition line. Then, the decrease in the derivative might be interpreted as a slight ordering of interstitial vortices prior to the major disordering upon melting. A similar feature has been observed in the structure factors in Monte Carlo simulations [21]. It is unclear, however, how these possible structural changes should affect the equilibrium magnetization. Also, on approaching a CP the FO induction step ΔB (and hence ΔS) is expected to vanish continuously. Figure 1(d) presents all the data points for the $B_\phi = 10$ G sample for which a clear ΔB could be resolved [open circles in Fig. 3(b)], which show only a mild decreasing tendency of ΔB near the CPs. Note that the intricate shape of dB/dH in the SO region complicates the quantitative data analysis in the vicinity of the CPs. Therefore, the locations of the CPs were determined quali-

tatively. Yet, 2 K (3 K) away from the lower (upper) CP the distinction between the FO peaks and the SO steps becomes unambiguous. Hence, the shown locations of the CPs have an accuracy of 2 to 3 K.

The FO transition line of irradiated samples persists to the left of its maximum in the inverse melting region (Fig. 3). These are the first equilibrium magnetization measurements in this region in presence of CDs. Figure 3(d) shows the phase diagram of a sample with $B_\phi = 20$ G and a slightly lower oxygen doping. This sample displays even more intricate behavior. Like the other $B_\phi = 20$ and 10 G samples, it also exhibits FO-SO-FO behavior. In addition, this sample reveals a third CP at low temperatures on the inverse melting side of the transition. Below this CP we observe a recurrence of the SO transition. It may be due to the fact that the melting field decreases in the inverse melting region with decreasing T. As a result, nanocrystals contain less vortices and correlated pinning regains dominance over elasticity. Consequently, the transition becomes SO once again, similarly to that at intermediate temperatures. Since the third CP occurs very close to the temperature below which our shaking equilibration becomes ineffective, this possible reoccurrence of the SO transition requires further study.

It is worth pointing out the qualitative difference between the behavior reported here and the SO-FO-SO sequence found in pristine samples of the less anisotropic YBCO compound [30]. In irradiated BSCCO all three portions of the transition line separate a solid phase from a liquid phase. In pristine YBCO, however, the high-field SO portion is believed to separate two liquid phases due to the existence of a tricritical point [31]. The low-field SO portion, on the other hand, separates a solid phase from a liquid phase and is believed to arise from the intrinsic disorder in YBCO crystals [25,32,33].

In summary, we present thermodynamic evidence for new FO-SO-FO behavior of the melting line in BSCCO with a low density of CDs. This unusual behavior is due to close competition between four different energy scales. As CDs are introduced, the melting transition initially alters its order from first to second at intermediate temperatures where correlated pinning has a dominant effect. At high and low temperatures the transition remains FO despite the disordering potential of CDs. At low temperatures where the melting field is high, the solid phase is dominated by elasticity rather than correlated pinning due to the increasing number of vortices per CD, and the FO transition is retained. The FO transition is likewise preserved at high temperatures, where correlated pinning is weakened by thermal fluctuations. As the density of the CDs is increased, the SO segment of the transition line expands both to the higher and lower temperatures. The observed nucleation and growth process of the SO segment clarifies the general process of transformation of phase transitions with increased disorder. In particular, it describes the mechanism that leads to transformation of a Bragg glass in the presence of point disorder to a BOG at high concentrations of correlated disorder, which melts through a single SO transition.

We thank C. J. van der Beek and M. Konczykowski for sample irradiation and Y. Y. Goldschmidt, E. H. Brandt, and G. P. Mikitik for useful discussions. This work was supported by the German Israeli Foundation (GIF), US-Israel BSF, and Grant-in-aid from the Ministry of Education, Culture, Sport, Science and Technology, Japan.

*tal.hazak@weizmann.ac.il

[1] Y. Imry and M. Wortis, Phys. Rev. B **19**, 3580 (1979).
[2] D. S. Fisher, M. P. A. Fisher, and D. A. Huse, Phys. Rev. B **43**, 130 (1991).
[3] E. Zeldov *et al.*, Nature (London) **375**, 373 (1995).
[4] T. Giamarchi and P. LeDoussal, Phys. Rev. B **52**, 1242 (1995).
[5] T. Nattermann, Phys. Rev. Lett. **64**, 2454 (1990).
[6] G. Blatter and V. B. Geshkenbein, *The Physics of Superconductors* (Springer, New York, 2003).
[7] N. Avraham *et al.*, Nature (London) **411**, 451 (2001).
[8] G. P. Mikitik and E. H. Brandt, Phys. Rev. B **68**, 054509 (2003).
[9] P. Olsson and S. Teitel, Phys. Rev. Lett. **87**, 137001 (2001).
[10] H. Beidenkopf *et al.*, Phys. Rev. Lett. **95**, 257004 (2005).
[11] D. R. Nelson and V. M. Vinokur, Phys. Rev. Lett. **68**, 2398 (1992).
[12] M. Konczykowski *et al.*, Physica C (Amsterdam) **408**, 547 (2004).
[13] B. Khaykovich *et al.*, Phys. Rev. B **57**, R14088 (1998); B. Khaykovich *et al.*, Physica C (Amsterdam) **282**, 2067 (1997).
[14] S. S. Banerjee *et al.*, Phys. Rev. Lett. **90**, 087004 (2003); S. S. Banerjee *et al.*, Phys. Rev. Lett. **93**, 097002 (2004).
[15] M. Menghini *et al.*, Phys. Rev. Lett. **90**, 147001 (2003).
[16] N. Avraham *et al.*, Phys. Rev. Lett. **99**, 087001 (2007).
[17] R. Ikeda, J. Phys. Soc. Jpn. **70**, 219 (2001).
[18] A. I. Larkin and V. M. Vinokur, Phys. Rev. Lett. **75**, 4666 (1995).
[19] L. Radzihovsky, Phys. Rev. Lett. **74**, 4923 (1995).
[20] J. P. Rodriguez, Phys. Rev. B **70**, 224507 (2004).
[21] S. Tyagi and Y. Y. Goldschmidt, Phys. Rev. B **67**, 214501 (2003); Y. Y. Goldschmidt and E. Cuansing, Phys. Rev. Lett. **95**, 177004 (2005); Y. Y. Goldschmidt and Jin-Tao Liu, Phys. Rev. B **76**, 174508 (2007).
[22] Y. Nonomura and X. Hu, Europhys. Lett. **65**, 533 (2004).
[23] C. Dasgupta *et al.*, Phys. Rev. B **72**, 094501 (2005).
[24] C. J. van der Beek *et al.*, Phys. Rev. Lett. **86**, 5136 (2001).
[25] M. Willemin *et al.*, Phys. Rev. Lett. **81**, 4236 (1998).
[26] G. P. Mikitik and E. H. Brandt, Phys. Rev. B **69**, 134521 (2004); Supercond. Sci. Technol. **20**, L9 (2007).
[27] B. Hayani *et al.*, Phys. Rev. B **61**, 717 (2000).
[28] R. J. Drost *et al.*, Phys. Rev. B **58**, R615 (1998).
[29] S. Colson *et al.*, Phys. Rev. B **69**, 180510 (2004).
[30] A. Schilling *et al.*, Phys. Rev. Lett. **78**, 4833 (1997).
[31] F. Bouquet *et al.*, Nature (London) **411**, 448 (2001).
[32] T. Nishizaki *et al.*, J. Phys. Conf. Ser. **51**, 267 (2006).
[33] W. K. Kwok *et al.*, Phys. Rev. Lett. **84**, 3706 (2000).